Novel Fat Depot–Specific Mechanisms Underlie Resistance to Visceral Obesity and Inflammation in 11β-Hydroxysteroid Dehydrogenase Type 1–Deficient Mice

Malgorzata Wamil,[1] Jenny H. Battle,[1,2] Sophie Turban,[2] Tiina Kipari,[1] David Seguret,[2] Ricardo de Sousa Peixoto,[1] Yvonne B. Nelson,[2] Dominika Nowakowska,[1,2] David Ferenbach,[3] Lynne Ramage,[2] Karen E. Chapman,[1] Jeremy Hughes,[3] Donald R. Dunbar,[4] Jonathan R. Seckl,[1] and Nicholas M. Morton[2]

Downloaded from http://diabetes.diabetesjournals.org/diabetes/article-pdf/60/4/1158/401369/1158.pdf by guest on 24 April 2024

OBJECTIVE—The study objective was to determine the key early mechanisms underlying the beneficial redistribution, function, and inflammatory profile of adipose tissue in 11β-hydroxysteroid dehydrogenase type 1 knockout (11β-HSD1$^{-/-}$) mice fed a high-fat (HF) diet.

RESEARCH DESIGN AND METHODS—By focusing on the earliest divergence in visceral adiposity, subcutaneous and visceral fat depots from 11β-HSD1$^{-/-}$ and C57Bl/6J control mice fed an HF diet for 4 weeks were used for comparative microarray analysis of gene expression, and differences were validated with real-time PCR. Key changes in metabolic signaling pathways were confirmed using Western blotting/immunoprecipitation, and fat cell size was compared with the respective chow-fed control groups. Altered adipose inflammatory cell content and function after 4 weeks (early) and 18 weeks (chronic) of HF feeding was investigated using fluorescence (and magnetic)-activated cell sorting analysis, immunohistochemistry, and in situ hybridization.

RESULTS—In subcutaneous fat, HF-fed 11β-HSD1$^{-/-}$ mice showed evidence of enhanced insulin and β-adrenergic signaling associated with accretion of smaller metabolically active adipocytes. In contrast, reduced 11β-HSD1$^{-/-}$ visceral fat accumulation was characterized by maintained AMP kinase activation, not insulin sensitization, and higher adipocyte interleukin-6 release. Intracellular glucocorticoid deficiency was unexpectedly associated with suppressed inflammatory signaling and lower adipocyte monocyte chemoattractant protein-1 secretion with strikingly reduced cytotoxic T-cell and macrophage infiltration, predominantly in visceral fat.

CONCLUSIONS—Our data define for the first time the novel and distinct depot-specific mechanisms driving healthier fat patterning and function as a result of reduced intra-adipose glucocorticoid levels. ***Diabetes*** **60:1158–1167, 2011**

From the [1]Endocrinology Unit, University of Edinburgh, Queen's Medical Research Institute, Edinburgh, Scotland; the [2]Molecular Metabolism Group, Centre for Cardiovascular Science, University of Edinburgh, Queen's Medical Research Institute, Edinburgh, Scotland; the [3]Centre for Inflammation Research, University of Edinburgh, Queen's Medical Research Institute, Edinburgh, Scotland; and the [4]Bioinformatics Core, CVS, University of Edinburgh, Queen's Medical Research Institute, Edinburgh, Scotland.

Corresponding author: Nicholas M. Morton, nik.morton@ed.ac.uk.

Received 14 June 2010 and accepted 20 January 2011.

DOI: 10.2337/db10-0830

This article contains Supplementary Data online at http://diabetes.diabetesjournals.org/lookup/suppl/doi:10.2337/db10-0830/-/DC1.

M.W., J.H.B., and S.T. contributed equally to this work.

© 2011 by the American Diabetes Association. Readers may use this article as long as the work is properly cited, the use is educational and not for profit, and the work is not altered. See http://creativecommons.org/licenses/by-nc-nd/3.0/ for details.

Accumulation of visceral fat strongly increases the risk of cardiometabolic disease, whereas peripheral fat accretion is relatively protective (1–3). Pronounced visceral adiposity, loss of subcutaneous adipose tissue, and metabolic disease typify rare Cushing's syndrome of plasma glucocorticoid excess. However, rather than high circulating glucocorticoid levels, in idiopathic obesity/metabolic syndrome there are high adipose tissue levels of 11β-hydroxysteroid dehydrogenase type 1 (11β-HSD1) that catalyze intracellular regeneration of active glucocorticoids from the inert circulating 11-keto forms (4,5). Consequently, local intra-adipose glucocorticoid regeneration may explain the phenotypic similarities between "Cushingoid" and idiopathic obesity (4,5). Indeed, transgenic overexpression of 11β-HSD1 selectively in adipose tissue recapitulates the major features of the metabolic syndrome (visceral obesity, insulin-resistant diabetes, dyslipidemia, hypertension), whereas ectopic adipose-selective expression of the glucocorticoid-inactivating 11β-hydroxysteroid dehydrogenase type 2 isoform attenuates metabolic syndrome (6–8). Consistent with this, 11β-HSD1 knockout (11β-HSD1$^{-/-}$) mice chronically fed a high-fat (HF) diet resist metabolic syndrome in part by preferentially accumulating peripheral rather than visceral fat (9).

Chronic inflammation of the adipose tissue is another prominent feature of obesity that drives subsequent disease (10). Elevated free fatty acid and adipocytokine levels impair adipose, liver, and muscle insulin signaling through stimulation of inflammation- and cellular stress-associated transcriptional cascades (10–13). Further, there is pronounced recruitment of proinflammatory cells, initially cytotoxic T-cells and subsequently macrophages into adipose tissue (particularly visceral) in obesity, which produce many of the cytokines/chemokines associated with insulin resistance (14–19).

The elevated 11β-HSD1 that is characteristic of adipose tissue in obesity (4,5) thus presents an intriguing paradox. Glucocorticoids have potent anti-inflammatory effects (20,21), and elevated 11β-HSD1 might feasibly curtail inflammatory signaling within the adipocytes and, through paracrine spillover (22), dampen neighboring proinflammatory cell function. The therapeutic insulin-sensitizing effect of 11β-HSD1 inhibition on adipocytes (9) might therefore be confounded by exacerbating local inflammation in vivo. Moreover, 11β-HSD1 is expressed in macrophages and is

increased by acute inflammatory stimuli (23–25) where glucocorticoids drive anti-inflammatory, proresolution effects (26,27). Indeed, 11β-HSD1$^{-/-}$ mice exhibited both a delayed resolution of inflammatory processes (24) and a more rapid and severe acute inflammatory response (25,28). Because inhibition of 11β-HSD1 is now in late-stage clinical development as a therapeutic strategy for the treatment of obesity (29), it is critical to determine whether 11β-HSD1 deficiency also exacerbates chronic inflammation of adipose tissue in obesity. To determine the basis of the favorably altered fat distribution and address the inflammatory paradox in 11β-HSD1$^{-/-}$ mice, we analyzed the fat depot–specific molecular, cellular, and adipokine secretory mechanisms underlying disease protection from exposure to an HF diet.

RESEARCH DESIGN AND METHODS

Materials. Antibodies were against insulin receptor substrate (IRS)-1 and p85-PI3K (Upstate Biotechnology, New York, NY). Akt, phospho-Akt (Ser 473), phospho-tyrosine, AMP-activated protein kinase (AMPK)α, phospho-AMPK (Thr 172), horseradish peroxidase anti-rabbit, and anti-mouse IgG were obtained from Cell Signaling Technology (Beverly, MA). Protein A-sepharose was obtained from Amersham (Little Chalfont, U.K.). Routine reagents were obtained from Sigma-Aldrich (Suffolk, U.K.).

Animals. All experiments were approved by The University of Edinburgh ethical committee and were according to the U.K. Animals (Scientific Procedures) Act 1986. Twelve-week-old male 11β-HSD1$^{-/-}$ mice (9) from >10 generations of backcross with C57Bl/6J were used. Mice were fed an HF diet (Research Diets D12331) for 4, 10, or 18 weeks. Subcutaneous (from around the thigh), mesenteric (visceral) fat and liver were dissected and frozen rapidly in liquid nitrogen. Our choice of peripheral fat was refined in this study to the more translational subcutaneous depot. Plasma glucose (Sigma HK assay, Sigma-Aldrich) and insulin (Crystal Chem ELISA, Crystal Chem Inc., Downers Grove, IL) were measured after a 6-h fast.

Microarray. Adipose RNA was prepared using Qiagen RNeasy kits (Venlo, the Netherlands) and hybridized to Affymetrix Mouse Genome 430 2.0 GeneChips (n = 5 per group), and differential expression was determined using the Bioconductor Limma tool and the Benjamini and Hochberg false discovery rate method. WebGestalt (http://bioinfo.vanderbilt.edu/webgestalt) and the Ingenuity Pathways Analysis program (http://www.ingenuity.com/index.html) were used to analyze the gene cluster functions with >1.5-fold genotype differential expression. Data are deposited in ArrayExpress under the accession number E-MEXP-1636.

Quantitative RT-PCR. By using oligo(dT)20 primer and Superscript III (Invitrogen, Paisley, U.K.), 1 μg of total RNA used was reverse transcribed. Expression of mRNA was quantitated by Light Cycler 480 RT-PCR (Roche, Burgess Hill, U.K.) with inventoried probes and primer sets (Applied Biosystems, Warrington, U.K.) normalized against the TATA-binding protein or actin level.

Insulin signaling in vivo and Western blotting. Mice fasted 6 h were injected i.p. with 0.75 mU/g body wt humulinS (Novo Nordisk, Crawley, U.K.) or saline. Fat depots and liver were dissected after 15 min, snap-frozen, and stored at −80°C. Tissues were homogenized in ice-cold lysis buffer (50 mmol/L Tris, pH 7.4, 0.27 mol/L sucrose, 1 mmol/L Na-orthovanadate, pH 10, 1 mmol/L EDTA, 1 mmol/L EGTA, 10 mmol/L Na β-glycerophosphate, 50 mmol/L NaF, 5 mmol/L Na pyrophosphate, 1% [w/v] Triton X-100, 0.1% [v/v] 2-mercaptoethanol, 1 tablet of complete TM protease inhibitor [Roche, Hertfordshire, U.K.]), and 50 μg of protein were run on 4–12% Bis-Tris gels for Western blotting. Protein signals were visualized using enhanced chemiluminescence (Pierce Biotechnology, Rockford, IL) by exposure to Amersham HyperfilmTH ECL film (Amersham) or with secondary goat anti-rabbit Alexa Fluor 700 IgG and IR Dye 800 donkey anti-mouse (Invitrogen, U.K.) using a Li-Cor Odyssey infrared imaging system.

Fat cell size. Adipocyte number was determined by counting 20 randomly selected areas in sections from mesenteric and subcutaneous fat depot of 11β-HSD1$^{-/-}$ mice and wild-type mice fed chow or HF diet (10 weeks) using Imagepro Plus (Mediacybernetics, Beech House, U.K.). The marker was blind to genotype.

Adipose tissue fractionation. Adipose tissues without lymph nodes were digested in Krebs–Ringer solution with 2 mg/mL collagenase type I (Worthington Biochemicals, NJ) at 37°C, shaken in an incubator for 1 h, filtered through 200-μmol/L mesh, and centrifuged to separate adipocytes from stromal vascular cells (SVCs). SVC fractions were refiltered to single-cell suspension through 100-μmol/L mesh and then 30-μmol/L mesh. Erythrocytes were lysed in 1 mL erythrocyte lysis buffer (Sigma Aldrich, Dorset, U.K.) for 5 min at room temperature.

Flow cytometry. For flow cytometry, 1×10^5 cells were preincubated in 100 μL PBS with 1 μg/mL FcR block (BD Biosciences, Oxford, U.K.) and then incubated with 0.2 μg each of rat anti-mouse–F4/80 APC, -CD11b FITC, and hamster anti-mouse-CD11c PE (Caltag, Invitrogen, Paisley, U.K.) in PBS with 10% mouse serum (Sigma Aldrich, Dorset, U.K.) for 30 min at 4°C in the dark. For T-cells, we used CD45-PerCPC5.5 (BD Biosciences) CD3-PE, CD4-PerCPCy5.5 (Biolegend, San Diego, CA), and CD8a-APC and CD4-FITC (eBioscience Inc., San Diego, CA). We found that collagenase digestion of SVC (and spleen) cleaved the CD4 moiety from the cells and therefore use CD3$^+$CD8$^-$ cells to infer the CD4$^+$ population in SVC preparations. Because genotype differences were mainly in the CD8$^+$ population, we did not pursue the CD4$^+$ subpopulations further in this study. Cells were sorted using a FACScalibur (BD Biosciences) flow cytometer and analyzed using Flowjo8.0 software (Treestar Inc., Ashland, OR).

Magnetic cell sorting. SVCs (10^7) were suspended in 90 μL magnetic cell sorting buffer (PBS w/o Ca^{2+} Mg^{2+}, 0.5% BSA, 2 mmol/L EDTA) with 10 μL of anti-mouse CD11b microbeads (Miltenyi Biotech, Surrey, U.K.) and incubated for 30 min at 4°C. Washed cells were separated using a MACS column mini separator (Miltenyi Biotech), where CD11b$^+$ cells (macrophages) and CD11b$^-$ cells (SVC) were collected separately. Macrophage enrichment (~85%) was verified by flow cytometry for CD11b$^+$ and F4/80$^+$, and cells were used for RNA isolation.

In situ hybridization. Frozen adipose sections were mounted onto Superfrost Plus slides and stored at −80°C. A 644-base pair F4/80 cDNA fragment was cloned into a T7 and SP6 promoter plasmid (Clontech, Oxford, U.K.) to make ^{35}S[UTP] (Amersham) labeled sense/antisense mRNA probes. Adipose sections were paraformaldehyde-fixed (4%) and hybridized with probe overnight at 50°C. Slides were washed, dried, and exposed to autoradiographic film for 7 days at room temperature. Expression was quantified with Image-Pro Plus by integrating signal from 20 random areas per tissue section.

Adipocyte cytokine secretion. Equal volumes of fractionated adipocytes and Dulbecco's modified Eagle's medium (Lonza, Berkshire, U.K.) with 10% FCS were mixed, and 400-μL aliquots were incubated as ceiling cultures for 16 or 24 h at 37°C, 5% CO_2. Cytokine secretion was determined by sandwich ELISA (R & D Systems, Abingdon, U.K.) for monocyte chemoattractant protein (MCP)-1 and interleukin (IL)-6, and by Cytometric Bead Array (BD Biosciences) for tumor necrosis factor (TNF)α and IL-10 and normalized to total adipocyte protein.

Cell culture. Mouse 3T3-L1 preadipocyte cells (30) were incubated in charcoal-stripped FBS-Dulbecco's modified Eagle's medium overnight before IL-6 treatments (24 h) before protein extraction and Western blotting.

Statistical analysis. Data were expressed as means ± SEM. For statistical analysis, the groups were compared using a two-way ANOVA as stated or by Student t test where stated. The Shapiro–Wilk W test (GraphPad Prism) was used to test for normal distribution. $P < 0.05$ was considered as significant.

RESULTS

Reduced fat mass in HF-fed 11β-HSD1$^{-/-}$ mice. Despite similar basal metabolic phenotypes (9), after 4 weeks of HF feeding, 11β-HSD1$^{-/-}$ mice exhibited a generalized reduction in fat mass gain, with a trend in the subcutaneous depot (−22%) but significantly lower mesenteric fat depot mass (−27%) and lower fasting glucose and insulin levels than congenic C57Bl/6J controls (Table 1).

Differential expression of genes in subcutaneous and mesenteric fat depot: overall analysis. We examined underlying gene expression differences at this early stage of divergence in (visceral) adiposity. Microarray revealed that 565 (subcutaneous) and 1,622 (mesenteric) transcripts were differentially expressed between genotypes ≥1.5-fold. HF-fed 11β-HSD1$^{-/-}$ mice showed mainly upregulation (79% genes) in subcutaneous but suppression (73% of genes) in mesenteric fat (Supplementary Tables 1 and 2, full data are deposited in the ArrayExpress database).

Genes expressed at higher levels in the subcutaneous fat of HF-fed 11β-HSD1$^{-/-}$ mice. Gene ontology analysis revealed the most significantly affected pathways included insulin signaling, β-adrenergic signaling, glucose metabolism (glycolysis), lipid metabolism (lipolysis, β-oxidation), oxidative phosphorylation, mitogen-activated protein/extracellular

Downloaded from http://diabetes.diabetesjournals.org/diabetes/article-pdf/60/4/1158/401369/1158.pdf by guest on 24 April 2024

TABLE 1
Physiologic characteristics of 11β-HSD1$^{-/-}$ and control mice fed chow or HF diet for 4 weeks

Parameter	C57Bl/6J chow	C57Bl/6J HF	11β-HSD1$^{-/-}$chow	11β-HSD1$^{-/-}$HF
Body weight (g)	32.3 ± 1.5	38.7 ± 1.5**	32.7 ± 0.7	35.8 ± 0.5**
Cumulative weight gain (g)	1.13 ± 0.1	6.2 ± 0.7**	1.31 ± 0.1	3 ± 0.6**†
Mesenteric fat mass (mg/g body wt)	32.8 ± 2.82	2.65 ± 0.1*	39 ± 3.33	1.99 ± 0.1*†
Absolute weight (mg)		94 ± 5*		69 ± 6*†
Subcutaneous fat mass (mg/g body wt)	1.87 ± 0.16	4.2 ± 0.3*	1.720.17	3.4 ± 0.1*
Absolute weight (mg)	54.2 ± 3.97	157 ± 17**	51.4 ± 5.22	122 ± 9**
Liver mass (left lobe; mg/g body wt)	4.97 ± 0.1	4.8 ± 0.1	5.1 ± 0.1	4.76 ± 0.1
Absolute weight (mg)	145 ± 3.01	174 ± 7*	150.03 ± 5.01	165 ± 5*
Fasting glucose (mg/dL)	140.7 ± 12.3	211.5 ± 4.8**	165.4 ± 8.0	157.5 ± 3.4†††
Fasting insulin (pg/mL)	12.8 ± 4.6	18.3 ± 1.9**	10.6 ± 2.0	7 ± 1.1††
Corticosterone (nmol/L)	53.5 ± 13.8	44.3 ± 22	60.1 ± 18.5	56.2 ± 19

Adipose depot fat mass was assessed in C57Bl/6J (control) and 11β-HSD1$^{-/-}$ mice after 4 weeks exposure to chow or HF diet. Glucose and insulin were measured in plasma samples obtained after 6 h of fasting. Data are the means ± SE (n = 5–7) analyzed by two-way ANOVA. *$P < 0.05$. **$P < 0.01$ indicates a significant effect of diet. †$P < 0.05$, ††$P < 0.01$, and †††$P < 0.001$ indicate an effect of genotype within diet (interaction).

Downloaded from http://diabetes.diabetesjournals.org/diabetes/article-pdf/60/4/1158/401369/1158.pdf by guest on 24 April 2024

signal–related kinase (MAP/ERK) signaling, and calcium signaling (selected genes shown in Supplementary Table 1).

Genes expressed at lower levels in the subcutaneous fat of HF-fed 11β-HSD1$^{-/-}$ mice. Among 23 genes expressed at lower levels in subcutaneous fat of HF-fed 11β-HSD1$^{-/-}$ mice were growth hormone receptor (−3.28-fold) and leptin (−1.66-fold), consistent with glucocorticoid regulation (9,31).

Genes expressed at lower levels in the mesenteric fat of HF-fed 11β-HSD1$^{-/-}$ mice. Genes suppressed in mesenteric fat of HF-fed 11β-HSD1$^{-/-}$ mice were related to immune cell trafficking, nuclear factor-κB, stress-activated protein kinase/Jun NH2-terminal kinase (SAPK/JNK), Jak/STAT signaling, chemokines, and TNF receptor-related family members, many of which are associated with inflammatory cellular stress and insulin resistance (10–19) in obesity/diabetes (selected genes are shown in Supplementary Table 2).

Genes expressed at higher levels in the mesenteric fat of HF-fed 11β-HSD1$^{-/-}$ mice. Genes upregulated in the mesenteric fat of HF-fed 11β-HSD1$^{-/-}$ mice included regulators of sarcoendoplasmic reticulum Ca^{2+}-ATPase activity (*Pln*, 2.25-fold, *Kcnk2*, 2.63-fold), retinol binding protein-transthyretin (2.3-fold), neurotransmitters *Vip* (2-fold) and tachykinin (2-fold), and cell surface receptors *Gnao1*, *Htr2b*, *Gpr85*, *Cap2*, *Tac1*, and *Galr2*.

Microarray quantitative RT-PCR validation. Microarray changes were validated to check for diet and depot-specificity of the highlighted pathways. Higher subcutaneous fat expression of the adipogenic insulin-sensitizing *Pparγ*, insulin-sensitive glucose transporter *Glut4*, oxidative AMP kinase subunit *Prkaa2*, lipid oxidizing *Cpt1b*, a target for 11β-HSD1 inhibitors (32), and adrenergic signaling-related *Hspb6* (33) were confirmed. Unexpectedly, *PPARγ* and *Prkaa2* were also elevated in mesenteric fat (Fig. 1*A*, Supplementary Table 3).

Functional validation of adipocyte peroxisome proliferator–activated receptor γ and adrenergic signaling. To test whether elevated peroxisome proliferator–activated receptor (PPAR)γ was of functional significance, we exposed subcutaneous adipocytes from HF-fed 11β-HSD1$^{-/-}$ mice to rosiglitazone and found higher basal levels of *Glut4* mRNA and a more marked *Glut4* induction by rosiglitazone (Supplementary Fig. 1).

To test for altered β-adrenergic signaling, we injected fasted C57BL/6J and 11β-HSD1$^{-/-}$ mice with the β3-agonist CL-316, 243 (CL: 0.33 nmol/g BW, n = 4) and measured nonesterified fatty acid release after 30 min. 11β-HSD1$^{-/-}$ mice exhibited a significantly greater increase from basal in plasma nonesterified fatty acid ($P < 0.01$) in response to the β3-agonist (C57BL/6J before CL: 0.62 ± 0.01 mEq/L, C57BL/6J after CL: 1.07 ± 0.002; 11β-HSD1$^{-/-}$ before CL 0.60 ± 0.02, 11β-HSD1$^{-/-}$ after CL: 1.13 ± 0.02).

Suppression of mesenteric fat cytotoxic T-cell (*Cd8*), chemokine signaling (*Stat4*), immunocyte adhesion (*L-selectin*), and macrophage/dendritic cell scavenger receptor (*Marco*) differences were confirmed by quantitative RT-PCR in only the HF-fed group (Fig. 1*B*, Supplementary Table 3).

11β-HSD1$^{-/-}$ subcutaneous fat has enhanced insulin signaling in vivo. The depot-selective insulin sensitization implied by differential *Glut4*, but not *PPARγ* expression, was assessed in vivo. Insulin-stimulated phosphorylation of IRS1, IRS-1 association with the p85 subunit of PI3K, and phosphorylation of AKT in subcutaneous fat were decreased in HF-fed control C57BL/6J (Fig. 2*A*) but not 11β-HSD1$^{-/-}$ mice. Indeed, AKT phosphorylation was maintained despite lower PI3K-associated IRS1 levels in the 11β-HSD1$^{-/-}$ mice in further support of increased insulin sensitization. Insulin signaling was comparable between genotypes in mesenteric fat with the HF diet (Fig. 2*B*) and in both depots with the chow diet (Supplementary Fig. 2).

11β-HSD1$^{-/-}$ visceral fat has activated AMPK. Despite higher *Prkaa2* (AMPKinase α2-subunit) mRNA in both fat depots of HF-fed 11β-HSD1$^{-/-}$ mice, AMPK activation (phosphorylation) was maintained only in the mesenteric fat of HF-fed 11β-HSD1$^{-/-}$ mice (Fig. 2*B*). Subcutaneous fat (HF-fed) phosphoAMPK/AMPK ratio was unchanged (C57BL/6J: 0.85 ± 0.11, 11β-HSD1$^{-/-}$: 0.83 ± 0.1).

Reduced subcutaneous adipocyte hypertrophy in 11β-HSD1$^{-/-}$ mice. To test for beneficial β-adrenergic/oxidative fat remodeling (34,35), we measured fat cell size after a 10-week HF diet. Cells per unit area (cpu) decreases as fat cell size increases. C57BL/6J mice showed a fivefold increase in subcutaneous fat cell size (chow: 64 ± 13 cpu, HF diet: 13 ± 2 cpu, $P < 0.001$), whereas 11β-HSD1$^{-/-}$ mice showed only a 2.5-fold increase (chow: 42 ± 10 cpu, HF diet: 17 ± 5 cpu, $P < 0.001$) despite comparable fat depot mass. Visceral fat cell hypertrophy was similar (~twofold increase) in both genotypes (C57BL/6J chow: 50 ± 5 cpu, HF diet: 20 ± 4 cpu, $P < 0.001$, 11β-HSD1$^{-/-}$ chow: 40 ± 9 cpu, HF diet: 19 ± 2 cpu, $P < 0.001$).

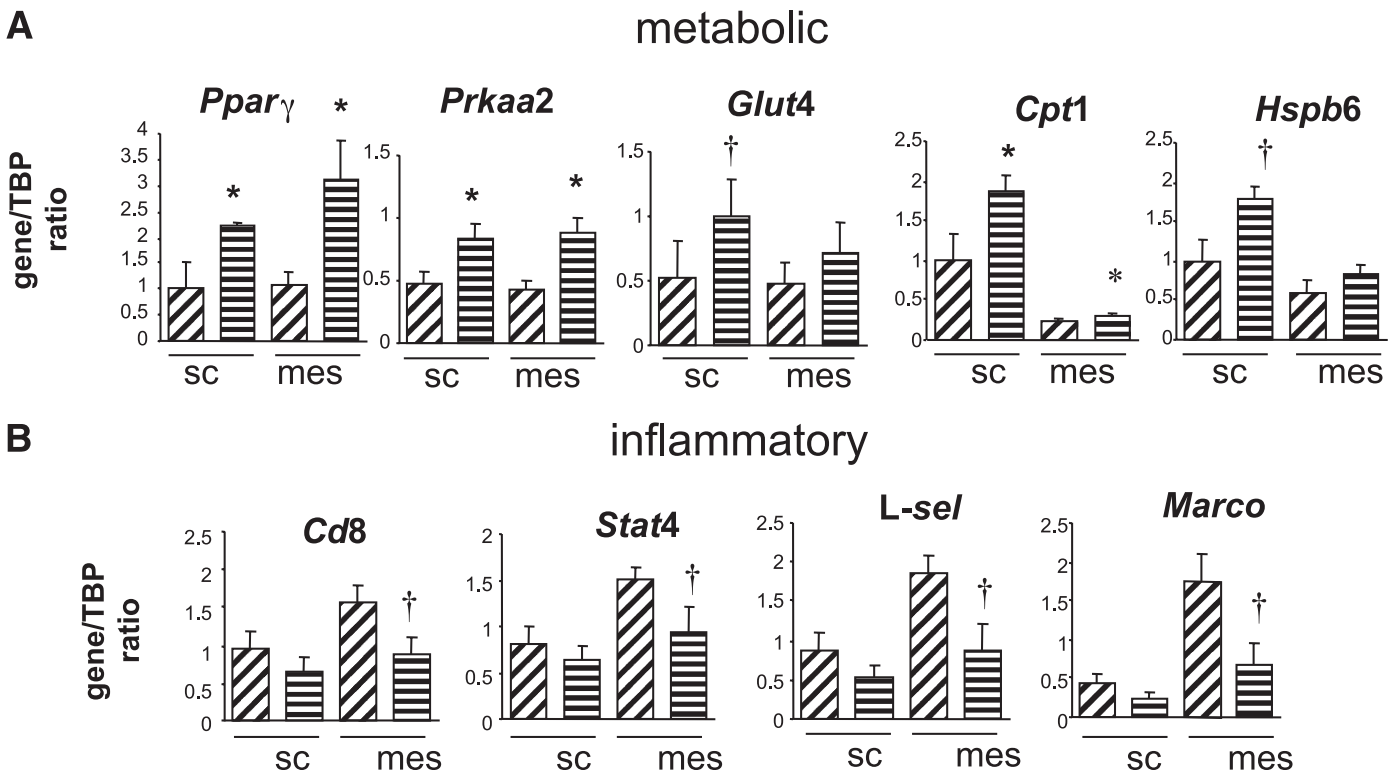

FIG. 1. Quantitative RT-PCR validation of microarray gene expression differences between HF-fed C57BL/6J and 11β-HSD1$^{-/-}$ adipose. C57BL/6J (▨) and 11β-HSD1$^{-/-}$ (▤) mice were fed an HF diet for 4 weeks. Levels of mRNA were measured in two fat depots: subcutaneous (sc) and mesenteric (mes). *A*: Representative genes involved in lipid and glucose metabolism altered in subcutaneous fat. *B*: Representative genes involved in inflammatory cell signaling and function altered in mesenteric fat. Data are presented as a mean ± SEM of two independent HF diet studies and are expressed as a ratio of the gene of interest to the TATA-binding protein internal control. *n* = 7–10. Analyses were by two-way ANOVA. Significant effects of genotype are shown: **P* < 0.05. Significant genotype-by-depot interaction is shown: †*P* < 0.05.

11β-HSD1$^{-/-}$ decreases T-cell infiltration of mesenteric fat. Cytotoxic CD8$^+$ T-cell infiltration is an early event in the inflammatory response of adipose tissue in obesity (17,19). Immunohistochemistry showed that CD3$^+$ cells (a general T-cell marker) were reduced in 11β-HSD1$^{-/-}$ mesenteric adipose tissue (Fig. 3*A*). Moreover, fluorescence-activated cell sorting analysis of the adipose SVCs showed that 11β-HSD1$^{-/-}$ mice had fewer CD8$^+$ T-cells irrespective of the dietary effect (Fig. 3*B*). SVC CD3$^+$CD8$^-$ cell numbers (a surrogate for T-helper CD4$^+$ cells) were comparable between genotypes (Fig. 3*B*). In contrast with the SVC, mesenteric fat-associated lymph node T-cell content (CD8$^+$ and CD4$^+$) was reduced in both genotypes with HF feeding (Fig. 3*C*), as described by others (36). Note the anti-CD4 fluorescence-activated cell sorting antibody used with lymph nodes as collagenase digestion (which removes CD4 antigen in SVC preparations) is not required.

Decreased macrophage infiltration into fat of 11β-HSD1$^{-/-}$ mice. Macrophage infiltration into adipose tissue (14–19) occurs as obesity develops. 11β-HSD1$^{-/-}$ mice had fewer visceral fat SVC macrophages on control diet (Fig. 4*A*). Moreover, 11β-HSD1$^{-/-}$ mice had significantly reduced macrophage infiltration into both subcutaneous and visceral adipose tissues after an 18-week HF diet (Fig. 4*B*). Similarly, in mice deficient in both leptin (genetically obese) and 11β-HSD1 (11β-HSD1$^{-/-}$-Lep^{ob} mice), there was reduced visceral fat macrophage infiltration (Fig. 4*C*) associated with reduced visceral fat mass (depot/body weight ratio: 11β-HSD1$^{-/-}$-Lep^{ob}: 0.0343 ± 0.001 vs. Lep^{ob}: 0.0384 ± 0.002, P = 0.017, n = 6) but not subcutaneous fat mass (11β-HSD1$^{-/-}$-Lep^{ob}: 0.0698 ± 0.008 vs. Lep^{ob}: 0.0681 ± 0.006).

Adipose macrophage 11β-HSD1 expression is unexpectedly decreased in obesity. 11β-HSD1 expression is induced in classically activated macrophages (23–25). We tested whether this also occurs in MACs-isolated adipose macrophages in obesity. 11β-HSD1 expression was highest in non-macrophage SVC cells (Fig. 5*A* and *B*), consistent with its expression in preadipocytes (30). Unexpectedly, HF-induced and genetic obesity (Lep^{ob}) were associated with low adipose tissue macrophage 11β-HSD1 expression (Fig. 5*A* and *B*, left).

Macrophage polarization into pro- (M1-type) or anti- (M2-type) inflammatory phenotypes is influenced by glucocorticoids and therefore possibly 11β-HSD1 (23–28). However, proinflammatory TNF-α, MCP1, migration inhibitory factor, IL-6, anti-inflammatory IL-10, and arginase I mRNA levels were comparable in adipose macrophages from 11β-HSD1$^{-/-}$ and C57BL/6J mice in both depots (Supplementary Table 4).

11β-HSD1$^{-/-}$ adipocytes secrete less MCP-1 but show depot-specific changes in IL-6 secretion. We next tested whether altered adipocyte adipokine secretion might drive reduced macrophage infiltration with an 18-week HF diet. MCP-1 secretion was significantly lower from 11β-HSD1$^{-/-}$ adipocytes regardless of depot or diet (11β-HSD1$^{-/-}$ mice: 32 ± 3 ng/μg/24 h vs. C57BL/6J mice: subcutaneous: 41 ± 2 ng/μg/24 h, mesenteric: 50 ± 4 ng/μg/24 h, P = 0.04). In addition, 11β-HSD1$^{-/-}$ subcutaneous adipocytes secreted less IL-6 (696 ± 37 pg/μg/24 h vs. C57BL6J control: 1,129 ± 175 pg/μg/24 h, P = 0.014), and this lower level was maintained

Downloaded from http://diabetes.diabetesjournals.org/diabetes/article-pdf/60/4/1158/401369/1158.pdf by guest on 24 April 2024

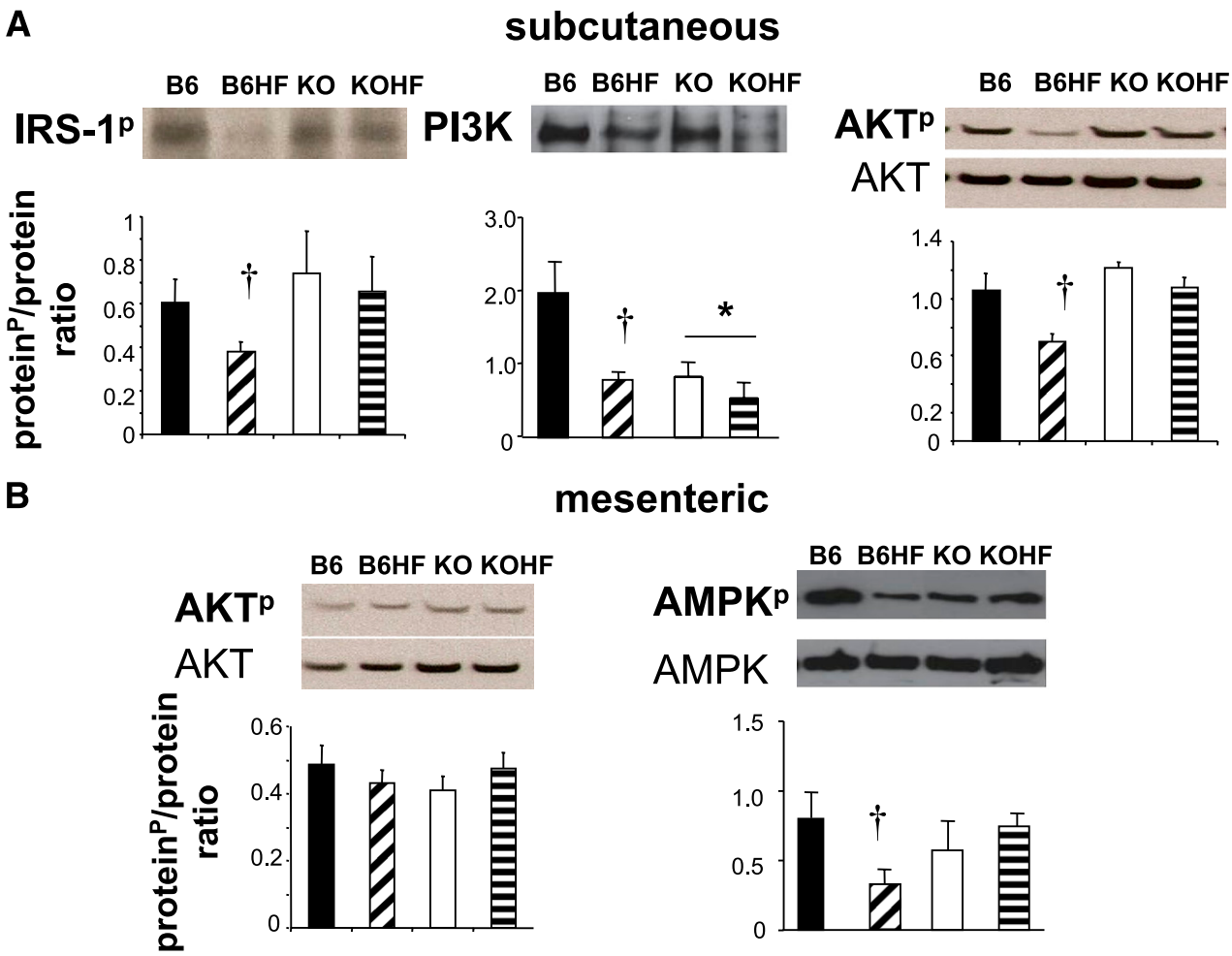

FIG. 2. Phosphorylation of proteins in the insulin and AMPK signaling pathways in adipose tissues of C57BL/6J and 11β-HSD1$^{-/-}$ mice. *A*: Immunoprecipitation using an anti-IRS1 antibody followed by Western blotting for IRS1-phosphotyrosine and *p*-85 PI3K and Western blot for phospho-AKTser473 (AKT^{p}) and pan-AKT (AKT) in insulin-treated C57BL/6J mice fed control (B6, ■) or HF (B6HF, ▨) diet and 11β-HSD1$^{-/-}$ mice on control (KO, □) or HF (KOHF, ▤) diet. *B*: Western blot for phospho/pan-AKT in mesenteric fat and for phospho-AMPKthr172 (AMPK^{p}) and pan-AMPK in mesenteric fat. n = 6–8. Effects of diet are shown as significant: †$P < 0.05$. Effects of genotype are shown as significant: *$P < 0.05$. (A high-quality color representation of this figure is available in the online issue.)

with the HF diet (699 ± 104 pg/μg/24 h). Similarly, IL-6 secretion was lower from 11β-HSD1$^{-/-}$ mesenteric adipocytes on control diet (615 ± 170 pg/μg/24 h vs. C57BL/6J control: 1015 ± 170 pg/μg/24 h). However, IL-6 secretion markedly increased with the HF diet in 11β-HSD1$^{-/-}$ mesenteric adipocytes (1069 ± 95 pg/μg/24 h, P = 0.028), whereas the HF diet reduced IL-6 secretion from C57BL/6J mesenteric adipocytes. Adipocyte TNF-α and IL-10 secretion were unaffected (Supplementary Table 5).

Glucocorticoids constrain IL-6–induced AMPK activation in adipocytes. To test whether adipocyte IL-6 secretion might link the pro-oxidative phenotype and increased AMPK activation in 11β-HSD1$^{-/-}$ mesenteric fat, we treated differentiated 3T3-L1 adipocytes in vitro with IL-6. IL-6–induced adipocyte AMPK phosphorylation was prevented by coincubation with the 11β-HSD1 substrate 11-DHC (Fig. 6).

DISCUSSION

This study focused on the critical early mechanisms underlying the metabolically protective adipose phenotype of HF-fed 11β-HSD1$^{-/-}$ mice. This derives from the following: *1*) PPARγ and β3-adrenergic-driven subcutaneous fat remodeling with more small, insulin-sensitized adipocytes; *2*) reduced visceral fat accumulation due to maintained AMPK kinase-mediated induction of lipid oxidation pathways; and *3*) reduced proinflammatory T-cell and macrophage infiltration into (predominantly visceral) fat.

Peripheral (e.g., subcutaneous) fat is intrinsically more insulin sensitive than visceral fat, and its accumulation offers relative metabolic protection (1–3). Conversely, visceral fat expresses higher levels of the glucocorticoid receptor (2,5,6), which may contribute to its reduced insulin sensitivity and exaggerated expansion in response to increased plasma cortisol (Cushing's syndrome) or adipose 11β-HSD1 (idiopathic obesity). These intrinsic differences likely shape the distinct depot-specific responses to PPARγ, adrenergic, and AMPK system activation. Although this has been inferred in previous work (9), we provide the first mechanistic evidence for insulin sensitization through PI3K, IRS1, and AKT in adipose tissue of 11β-HSD1$^{-/-}$ mice showing this is maintained only in peripheral fat on exposure to an HF diet. We show subcutaneous fat of 11β-HSD1$^{-/-}$ mice exhibits elevated *Glut4* that remains *PPARγ* agonist-inducible after the HF diet, which is consistent with depot-specific insulin sensitization.

Downloaded from http://diabetes.diabetesjournals.org/diabetes/article-pdf/60/4/1158/401369/1158.pdf by guest on 24 April 2024

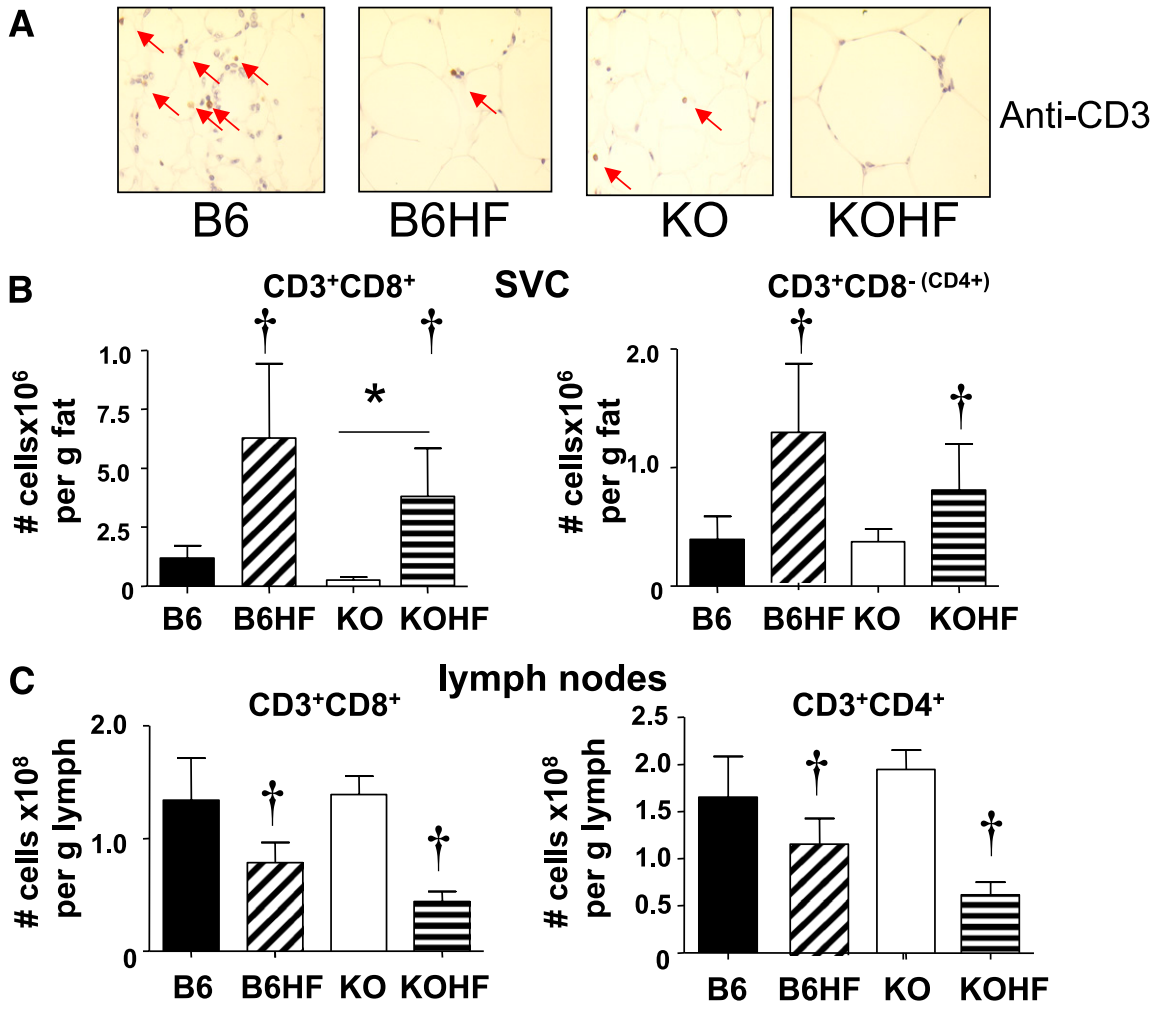

FIG. 3. T-cell levels in adipose tissues of C57BL/6J and 11β-HSD1$^{-/-}$ mice fed HF diet for 4 weeks. *A*: Anti-CD3 staining in mesenteric adipose sections from C57BL/6J (B6) and 11β-HSD1$^{-/-}$ mice (KO) fed control or HF diet (B6HF, KOHF) (representative of $n = 5$). Note fat cell expansion causes the appearance of lower CD3$^+$ cells/area, but there is actually an increase per depot as shown in *B*. FACS quantification of T-cell numbers in mesenteric (*B*) adipose SVC, and (*C*) adipose lymph nodes from C57BL/6J mice fed control (■) or HF (▨) diet and 11β-HSD1$^{-/-}$ mice fed control (□) or HF (▤) diet. CD8+ cytotoxic T-cells are shown on the *left*, and CD3$^+$CD8$^-$ (a surrogate for CD4$^+$ T-helper cells) FACS data are shown on the *right*; $n = 4$, with adipose pooled from two mice per condition. Effects of diet are shown as significant: †$P < 0.05$. Effects of genotype are shown as significant: *$P < 0.05$. (A high-quality digital representation of this figure is available in the online issue.)

This is consistent with both PPARγ induction (37) and glucocorticoid-mediated suppression of *Glut4* (38). Enhanced β-adrenergic remodeling may explain reduced fat cell size (34,35) with increased glucose uptake (39) of 11β-HSD1$^{-/-}$ subcutaneous fat. Glucocorticoids suppress adrenergic processes in (brown) fat (40), suggesting similar mechanisms may facilitate increased oxidative capacity of 11β-HSD1$^{-/-}$ white fat. Increased expression of CPT-1 and genes of oxidative phosphorylation in 11β-HSD1$^{-/-}$ adipose support this notion. Induction of *Hsp6* that protects cardiomyocytes from chronic (β-3) adrenergic induction of apoptosis (33) may similarly protect 11β-HSD1$^{-/-}$ adipocytes from increased cellular stress with an HF diet. The coexistence of elevated PPARγ and adrenergic signaling may seem contradictory given that PPARγ activation suppresses sympathetic drive to white and brown fat despite upregulating thermogenic components of the adrenergic system in vivo (41). We suggest that intra-adipose glucocorticoid deficiency in 11β-HSD1$^{-/-}$ may therefore not only drive increased expression of these distinct systems but also attenuate their functional antagonism. Of note, 11β-HSD1$^{-/-}$ mice on the C57BL/6J strain have increased hypothalamic glucocorticoid receptor levels and thus correct the HPA axis feedback deficiency seen in the original 129-based strain (42). Although this argues for a dominant effect of intra-adipose glucocorticoid deficiency as the underlying basis of healthier fat patterning, whether or not this corrective effect pertains to glucocorticoid control of the sympathetic system at the hypothalamic or brain stem level is uncertain.

11β-HSD1$^{-/-}$ mice showed elevated AMPK mRNA levels in both subcutaneous and visceral fat, but maintained AMPK phosphorylation (activation) only in visceral fat after the HF diet. PPARγ activation (43) and adrenergic stimulation (44) increase AMPK activation, whereas this is suppressed by glucocorticoids (45), suggesting that increased PPARγ sensitivity, presumably to the higher circulating free fatty acid PPARγ ligands with the HF diet, may be the underlying mechanism for the elevated AMPK. Notably, AMPK activity is inhibited by insulin (46), which seems the likely explanation for the lack of maintained AMPK phosphorylation—despite higher AMPK mRNA levels—in subcutaneous fat. This makes some teleologic sense, because AMPK signals for oxidation and lipid

Downloaded from http://diabetes.diabetesjournals.org/diabetes/article-pdf/60/4/1158/401369/1158.pdf by guest on 24 April 2024

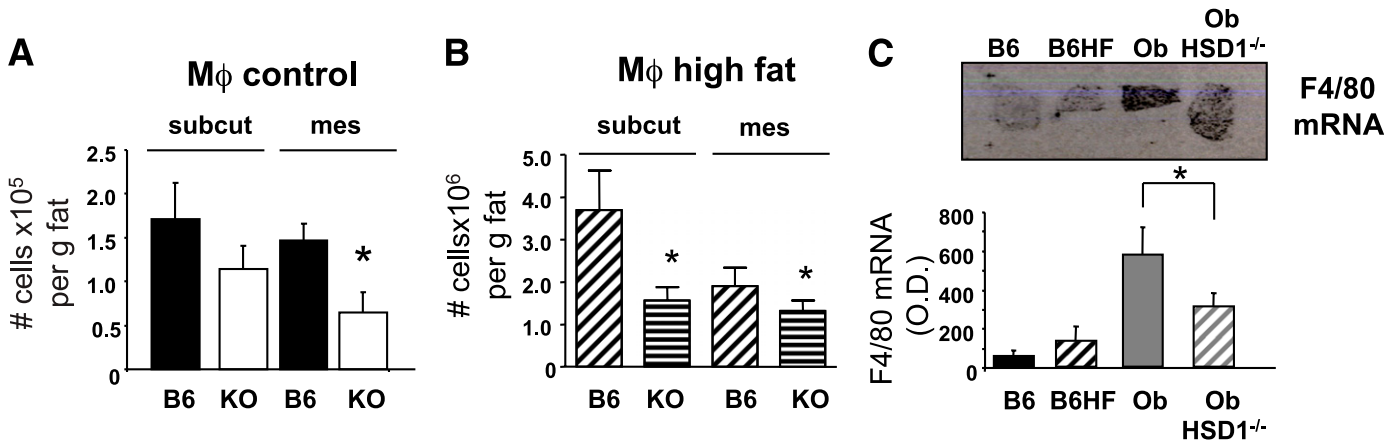

FIG. 4. Macrophage numbers in adipose tissues from C57BL/6J and 11β-HSD1$^{-/-}$ mice after 18-week HF diet. *A*: FACS quantification of total macrophages (Mϕ) content (Cd11b^{+}) in subcutaneous and mesenteric fat, as a percentage of the total SVC number, in C57BL/6J (■) or 11β-HSD1$^{-/-}$ mice (□) on control diet. *B*: FACS quantification of macrophage number (CD11b^{+}) as cells per gram of adipose tissue in subcutaneous and mesenteric fat after 18-week HF diet in C57BL/6J (▨) and 11β-HSD1$^{-/-}$ mice (▤); n = 6 with adipose pooled from two mice per condition. *C*: Quantitative results from in situ hybridization with an antisense riboprobe (*top*) hybridized against the macrophage marker F4/80 in mesenteric fat of C57BL/6J mice fed control (B6: ■) or HF (B6HF: ▨) diet and in genetically obese Lep*ob* mice (Ob: ■) and Lep*ob* mice that are 11β-HSD1 deficient (Ob HSD1$^{-/-}$: ▨); n = 6, effects of genotype are shown as significant: *$P < 0.05$. (A high-quality color representation of this figure is available in the online issue.)

mobilization, whereas insulin is anti-lipolytic and lipogenic in adipocytes. Activation of these opposing pathways is mutually exclusive in subcutaneous fat where 11β-HSD1$^{-/-}$ mice exhibit insulin sensitization. Notably, 11β-HSD1 inhibitors increase CPT-1–mediated oxidative drive in visceral adipose tissue, while driving lipogenic effects in peripheral-like fat of rats (32), further supporting a depot-specific effect of glucocorticoid deficiency.

The current work therefore provides a novel mechanistic framework for the early depot-specific responses to an HF diet resulting from intracellular glucocorticoid deficiency: combined adrenergic remodeling with insulin sensitization in peripheral fat and maintained AMPK-fat-oxidation in visceral fat. Although distinct, these effects are nevertheless consistent with a coordinated response through increased PPARγ action that drives a similar beneficial fat redistribution in rodents and humans (47,48). Given that the early generalized reduction in fat mass (4-week HF diet) of 11β-HSD1$^{-/-}$ mice is later followed by

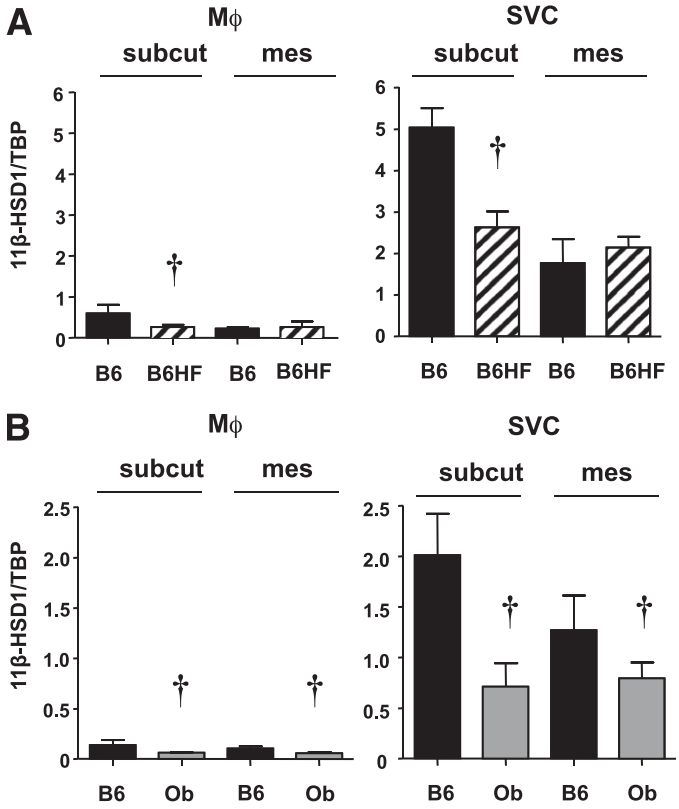

FIG. 5. 11β-HSD1 mRNA levels in MACS-enriched adipose macrophages from 18-week HF diet–induced and genetically obese mice. Adipose stromal macrophages (Mϕ) (CD11b^{+}, *left*) were enriched with magnetic-bead cell sorting using the anti-CD11b antibody from other SVCs (CD11b^{-}, *right*) in *A* the subcutaneous and mesenteric adipose tissues of C57BL/6J mice fed control (B6: ■) or HF (B6HF: ▨) diet or in *B* genetically obese Lep*ob* mice (Ob: ■). Effects of genotype (†) and diet (*) are shown as significant: $P < 0.05$.

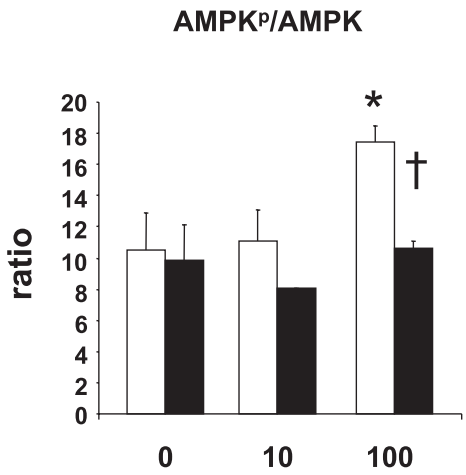

FIG. 6. 11β-HSD1 activity suppresses IL-6–mediated activation of AMP kinase in 3T3-L1 adipocytes. Differentiated 3T3-L1 adipocytes were exposed to increasing concentrations of IL-6 (□) alone or in the presence of the 11β-HSD1 substrate 11-DHC (200 nM, ■) for 24 h. Cells were homogenized, and levels of phosphorylated (activated) AMPK were determined by Western blot. *$P < 0.05$ for effects of 100 ng/mL IL-6 compared with basal and †$P < 0.05$ for effects of 11-DHC on IL-6–stimulated AMPK activation. Data are mean ± SEM, n = 4.

Downloaded from http://diabetes.diabetesjournals.org/diabetes/article-pdf/60/4/1158/401369/1158.pdf by guest on 24 April 2024

preferential peripheral fat accumulation (18-week HF diet), it may be that an early adrenergic, oxidative component is replaced by a dominant though still protective fat redistribution effect due to increased fatty acid flux-mediated PPARγ activation (Fig. 7). The exact sequence of events from glucocorticoid deficiency to increased PPARγ-related action will require further in-depth dissection but could suggest a therapeutic synergy between the two systems.

Maintained AMPK activation with an HF diet occurs alongside elevated 11β-HSD1$^{-/-}$ adipocyte IL-6 release. The role of IL-6 in insulin resistance is controversial (49). However, IL-6 activates (50) whereas glucocorticoids suppress (45) AMPK in adipocytes. We show IL-6–mediated AMPK activation is constrained by 11β-HSD1 activity in adipocytes, and this delineates a novel local mechanism constraining visceral fat accumulation with 11β-HSD1 deficiency. On the other hand, IL-6 secretion is lower from subcutaneous adipocytes of HF-fed 11β-HSD1$^{-/-}$ mice, where insulin sensitization predominates, and this may also contribute to reduced AMPK activation despite higher AMPK mRNA levels in this depot.

Visceral fat of HF-fed 11β-HSD1$^{-/-}$ mice expressed lower levels of genes involved in proliferation, differentiation, movement, and adhesion of immune cells, including T-cells. We confirmed reduced T-cell numbers in 11β-HSD1$^{-/-}$ visceral adipose, indicating beneficial regulation of the earliest inflammatory cell responses to HF feeding. Indeed, 11β-HSD1$^{-/-}$ mice have fewer resident adipose CD8+ T-cells and macrophages even on control diet. Although this suggests a role for adipose 11β-HSD1 in normal immune cell turnover and suppression, the manifestation of the protective effects of reduced immune cell burden only becomes apparent when the challenge of the HF diet induces insulin resistance and increases cell recruitment. Thus, reduced macrophage number contributes to the anti-inflammatory phenotype of 11β-HSD1$^{-/-}$ adipose and is likely to improve insulin sensitization, particularly at later stages of obesity. This is due in part to reduced macrophage recruitment as a result of lower adipocyte MCP1 secretion, rather than altered macrophage polarization. Because high-dose dexamethasone inhibits MCP1 secretion from clonal adipocytes in vitro (51), our findings may suggest secondary insulin sensitization or PPARγ action drives reduced adipose MCP1 secretion from 11β-HSD1$^{-/-}$ adipocytes, in agreement with the effects of 11β-HSD1 inhibition in vivo (52). Indeed, lower MCP-1 might also improve systemic insulin sensitivity (53) in 11β-HSD1$^{-/-}$ mice.

A recent comparison of gene expression patterns confirmed induction of 11β-HSD1 in macrophages that were classically (M1) rather than alternately (M2) activated (23). It was therefore unexpected that 11β-HSD1 levels were reduced in adipose tissue macrophages with dietary and

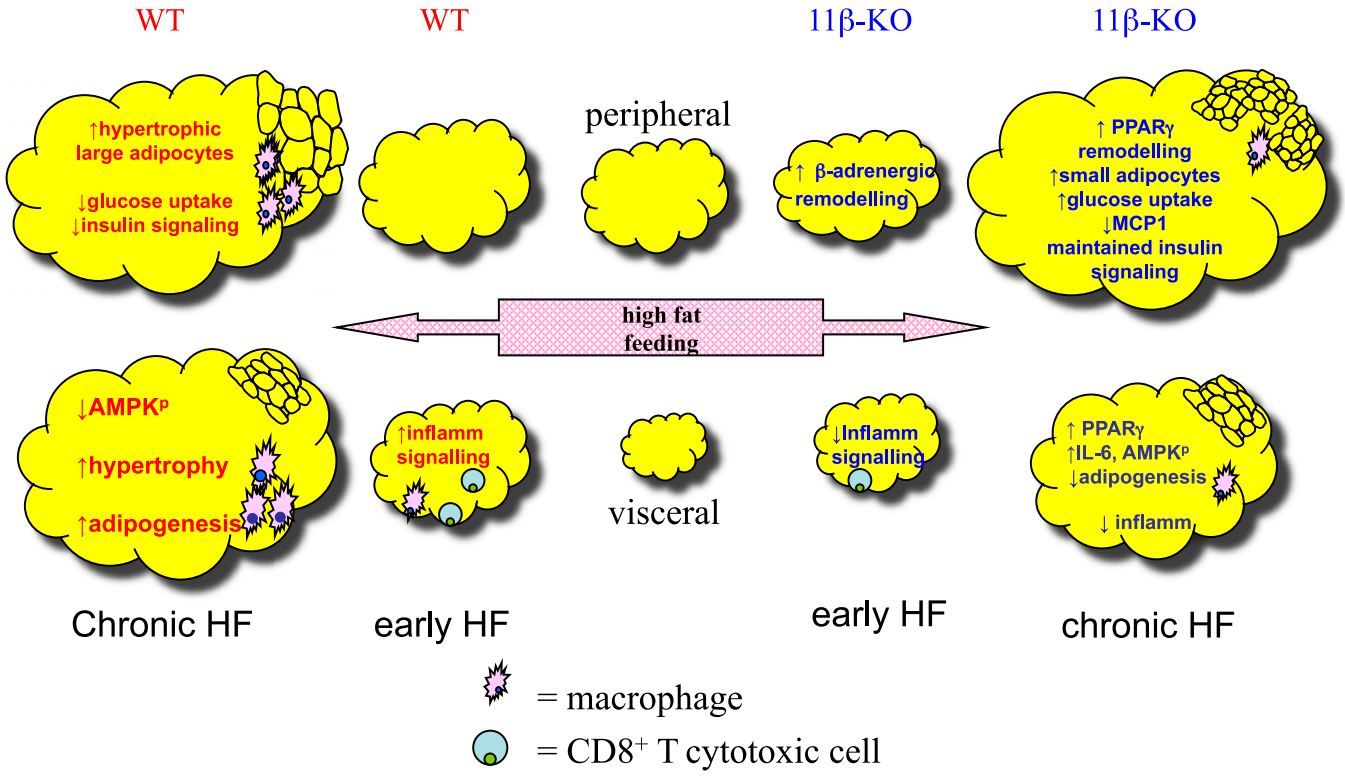

FIG. 7. Summary of the effects of 11β-HSD1 deficiency (low intracellular glucocorticoid action) on subcutaneous and visceral fat in obesity after early (4-week) and chronic (18-week) HF diet exposure. HF feeding causes a differential expansion of adipose mass (*pink double-sided arrow*) in the genotypes. After an initial period of generally attenuated fat mass accumulation (4-week HF diet), fat becomes favorably redistributed toward safer peripheral (subcutaneous) fat stores and away from detrimental visceral (mesenteric) fat stores in 11β-HSD1$^{-/-}$ mice (11β-KO) with chronic (18-week) HF diet (9). In subcutaneous fat, higher PPARγ (and β-adrenergic) remodeling drives increased numbers of small metabolically competent adipocytes that maintain insulin sensitivity, increased glucose uptake, and potentially oxidative drive, despite overall greater fat mass with chronic HF diet (9). In visceral fat, higher PPARγ and increased adipocyte IL-6 secretion drives maintained AMPK-mediated fat oxidation, independently of insulin sensitization. Reduced visceral fat inflammatory responses in 11β-HSD1$^{-/-}$ mice become accentuated with HF diet, particularly an early (4-week) reduction in CD8+ T-cells and a later reduction in macrophage content due, in part, to reduced adipocyte MCP1 secretion from 11β-HSD1$^{-/-}$ adipocytes. Visceral fat of 11β-HSD-1$^{-/-}$ mice also exhibits reduced adipogenesis (30). WT: C57BL/6J mice, 11β-KO: 11β-HSD1$^{-/-}$ mice.

Downloaded from http://diabetes.diabetesjournals.org/diabetes/article-pdf/60/4/1158/401369/1158.pdf by guest on 24 April 2024

genetic obesity, where macrophage activation occurs (10–15). Our data suggest two possibilities. First, 11β-HSD1 may be downregulated in a subpopulation of alternatively activated (M2-like) adipose macrophages, which also accumulate in diet-induced and genetic obesity (14). Second, the low-grade chronic activation of adipose macrophages that occurs in obesity is mechanistically distinct to that of acute classic inflammation and is not sufficient to induce the higher macrophage 11β-HSD1 expression associated with these more severe inflammatory insults (24,25).

Our data clarify early and novel pathways invoked by 11β-HSD1 deficiency that confer protection from visceral obesity and its consequent chronic adipose inflammation. We further demonstrate that the main protective contribution originates in the adipocytes and not the infiltrating macrophages. Our findings were transposable to a model of extreme genetic obesity (Lep^{ob}), indicating a beneficial impact of 11β-HSD1 deficiency in a wider context. Unexpectedly perhaps, adipose tissue macrophage 11β-HSD1 is reduced with obesity and does not seem to regulate macrophage polarization in this context. Crucially, our data imply that therapeutic inhibition of adipose 11β-HSD1 will not cause a potentially confounding exacerbation of adipose tissue inflammation in obesity.

ACKNOWLEDGMENTS

This research was supported by a British Heart Foundation 4-year PhD studentship (M.W.), a Wellcome Trust RCD Fellowship (N.M.M.), and a Wellcome Trust Programme Grant (J.R.S. and K.E.C.). D.R.D. was funded by the Wellcome Trust Functional Genomics and Cardiovascular Genomics Initiatives and by a British Heart Foundation CoRE award.

No potential conflicts of interest relevant to this article were reported.

M.W., J.H.B., S.T., T.K., D.S., R.d.S.P., Y.B.N., D.N., D.F., and L.R. researched data. K.E.C. and J.H. contributed to discussion. D.R.D. researched data. J.R.S. reviewed and edited the article. N.M.M. researched data and wrote the article.

The authors thank Dr. Pawel Herzyk and the microarray team at The Sir Henry Wellcome Functional Genomics Facility in Glasgow for processing samples; Dr. Kerry McInnes, Endocrinology Unit, Centre for Cardiovascular Sciences, University of Edinburgh, for advice on AMPK Western blots; and Margaret Ross, Endocrinology Unit, University of Edinburgh, for fat cell size measurements.

REFERENCES

1. Gabriely I, Ma XH, Yang XM, et al. Removal of visceral fat prevents insulin resistance and glucose intolerance of aging: an adipokine-mediated process? Diabetes 2002;51:2951–2958
2. Wajchenberg BL. Subcutaneous and visceral adipose tissue: their relation to the metabolic syndrome. Endocr Rev 2000;21:697–738
3. Jensen MD. Role of body fat distribution and the metabolic complications of obesity. J Clin Endocrinol Metab 2008;93(Suppl. 1):S57–S63
4. Tomlinson JW, Stewart PM. Mechanisms of disease: selective inhibition of 11beta-hydroxysteroid dehydrogenase type 1 as a novel treatment for the metabolic syndrome. Nat Clin Pract Endocrinol Metab 2005;1:92–99
5. Morton NM, Seckl JR. 11beta-hydroxysteroid dehydrogenase type 1 and obesity. Front Horm Res 2008;36:146–164
6. Masuzaki H, Paterson J, Shinyama H, et al. A transgenic model of visceral obesity and the metabolic syndrome. Science 2001;294:2166–2170
7. Masuzaki H, Yamamoto H, Kenyon CJ, et al. Transgenic amplification of glucocorticoid action in adipose tissue causes high blood pressure in mice. J Clin Invest 2003;112:83–90
8. Kershaw EE, Morton NM, Dhillon H, Ramage L, Seckl JR, Flier JS. Adipocyte-specific glucocorticoid inactivation protects against diet-induced obesity. Diabetes 2005;54:1023–1031
9. Morton NM, Paterson JM, Masuzaki H, et al. Novel adipose tissue-mediated resistance to diet-induced visceral obesity in 11 beta-hydroxysteroid dehydrogenase type 1-deficient mice. Diabetes 2004;53:931–938
10. Hotamisligil GS. Inflammation and metabolic disorders. Nature 2006;444:860–867
11. Tilg H, Moschen AR. Adipocytokines: mediators linking adipose tissue, inflammation and immunity. Nat Rev Immunol 2006;6:772–783
12. Yuan M, Konstantopoulos N, Lee J, et al. Reversal of obesity- and diet-induced insulin resistance with salicylates or targeted disruption of Ikkbeta. Science 2001;293:1673–1677
13. Hirosumi J, Tuncman G, Chang L, et al. A central role for JNK in obesity and insulin resistance. Nature 2002;420:333–336
14. Odegaard JI, Chawla A. Mechanisms of macrophage activation in obesity-induced insulin resistance. Nat Clin Pract Endocrinol Metab 2008;4:619–626
15. Weisberg SP, McCann D, Desai M, Rosenbaum M, Leibel RL, Ferrante AW Jr. Obesity is associated with macrophage accumulation in adipose tissue. J Clin Invest 2003;112:1796–1808
16. Xu H, Barnes GT, Yang Q, et al. Chronic inflammation in fat plays a crucial role in the development of obesity-related insulin resistance. J Clin Invest 2003;112:1821–1830
17. Wu H, Ghosh S, Perrard XD, et al. T-cell accumulation and regulated on activation, normal T cell expressed and secreted upregulation in adipose tissue in obesity. Circulation 2007;115:1029–1038
18. Nguyen MT, Favelyukis S, Nguyen AK, et al. A subpopulation of macrophages infiltrates hypertrophic adipose tissue and is activated by free fatty acids via Toll-like receptors 2 and 4 and JNK-dependent pathways. J Biol Chem 2007;282:35279–35292
19. Rausch ME, Weisberg S, Vardhana P, Tortoriello DV. Obesity in C57BL/6J mice is characterized by adipose tissue hypoxia and cytotoxic T-cell infiltration. Int J Obes (Lond) 2008;32:451–463
20. Gudbjornsson B, Juliusson UI, Gudjonsson FV. Prevalence of long term steroid treatment and the frequency of decision making to prevent steroid induced osteoporosis in daily clinical practice. Ann Rheum Dis 2002;61:32–36
21. Reichardt HM, Schütz G. Glucocorticoid signalling—multiple variations of a common theme. Mol Cell Endocrinol 1998;146:1–6
22. Stimson RH, Andersson J, Andrew R, et al. Cortisol release from adipose tissue by 11beta-hydroxysteroid dehydrogenase type 1 in humans. Diabetes 2009;58:46–53
23. Martinez FO, Gordon S, Locati M, Mantovani A. Transcriptional profiling of the human monocyte-to-macrophage differentiation and polarization: new molecules and patterns of gene expression. J Immunol 2006;177:7303–7311
24. Gilmour JS, Coutinho AE, Cailhier JF, et al. Local amplification of glucocorticoids by 11 beta-hydroxysteroid dehydrogenase type 1 promotes macrophage phagocytosis of apoptotic leukocytes. J Immunol 2006;176:7605–7611
25. Coutinho AE, Gray M, Sawatzky DA, et al. Deficiency in 11β-hydroxysteroid dehydrogenase type 1 results in a more rapid and severe inflammation. American Endocrine Society Abstract 2008:2–8
26. Heasman SJ, Giles KM, Ward C, Rossi AG, Haslett C, Dransfield I. Glucocorticoid-mediated regulation of granulocyte apoptosis and macrophage phagocytosis of apoptotic cells: implications for the resolution of inflammation. J Endocrinol 2003;178:29–36
27. Varga G, Ehrchen J, Tsianakas A, et al. Glucocorticoids induce an activated, anti-inflammatory monocyte subset in mice that resembles myeloid-derived suppressor cells. J Leukoc Biol 2008;84:644–650
28. Zhang TY, Daynes RA. Macrophages from 11beta-hydroxysteroid dehydrogenase type 1-deficient mice exhibit an increased sensitivity to lipopolysaccharide stimulation due to TGF-beta-mediated up-regulation of SHIP1 expression. J Immunol 2007;179:6325–6335
29. Hughes KA, Webster SP, Walker BR. 11-Beta-hydroxysteroid dehydrogenase type 1 (11beta-HSD1) inhibitors in type 2 diabetes mellitus and obesity. Expert Opin Investig Drugs 2008;17:481–496
30. De Sousa Peixoto RA, Turban S, Battle JH, Chapman KE, Seckl JR, Morton NM. Preadipocyte 11beta-hydroxysteroid dehydrogenase type 1 is a ketoreductase and contributes to diet-induced visceral obesity in vivo. Endocrinology 2008;149:1861–1868
31. Beauloye V, Ketelslegers JM, Moreau B, Thissen JP. Dexamethasone inhibits both growth hormone (GH)-induction of insulin-like growth factor-I (IGF-I) mRNA and GH receptor (GHR) mRNA levels in rat primary cultured hepatocytes. Growth Horm IGF Res 1999;9:205–211
32. Berthiaume M, Laplante M, Festuccia W, et al. Depot-specific modulation of rat intraabdominal adipose tissue lipid metabolism by pharmacological

Downloaded from http://diabetes.diabetesjournals.org/diabetes/article-pdf/60/4/1158/401369/1158.pdf by guest on 24 April 2024

inhibition of 11beta-hydroxysteroid dehydrogenase type 1. Endocrinology 2007;148:2391–2397
33. Fan GC, Chu G, Mitton B, Song Q, Yuan Q, Kranias EG. Small heat-shock protein Hsp20 phosphorylation inhibits beta-agonist-induced cardiac apoptosis. Circ Res 2004;94:1474–1482
34. Himms-Hagen J, Melnyk A, Zingaretti MC, Ceresi E, Barbatelli G, Cinti S. Multilocular fat cells in WAT of CL-316243-treated rats derive directly from white adipocytes. Am J Physiol Cell Physiol 2000;279:C670–C681
35. Granneman JG, Li P, Zhu Z, Lu Y. Metabolic and cellular plasticity in white adipose tissue I: effects of beta3-adrenergic receptor activation. Am J Physiol Endocrinol Metab 2005;289:E608–E616
36. Kim CS, Lee SC, Kim YM, et al. Visceral fat accumulation induced by a high-fat diet causes the atrophy of mesenteric lymph nodes in obese mice. Obesity (Silver Spring) 2008;16:1261–1269
37. Hauner H. The mode of action of thiazolidinediones. Diabetes Metab Res Rev 2002;18(Suppl. 2):S10–S15
38. Ngo S, Barry JB, Nisbet JC, Prins JB, Whitehead JP. Reduced phosphorylation of AS160 contributes to glucocorticoid-mediated inhibition of glucose uptake in human and murine adipocytes. Mol Cell Endocrinol 2009; 302:33–40
39. de Souza CJ, Hirshman MF, Horton ES. CL-316,243, a beta3-specific adrenoceptor agonist, enhances insulin-stimulated glucose disposal in nonobese rats. Diabetes 1997;46:1257–1263
40. Soumano K, Desbiens S, Rabelo R, Bakopanos E, Camirand A, Silva JE. Glucocorticoids inhibit the transcriptional response of the uncoupling protein-1 gene to adrenergic stimulation in a brown adipose cell line. Mol Cell Endocrinol 2000;165:7–15
41. Festuccia WT, Oztezcan S, Laplante M, et al. Peroxisome proliferator-activated receptor-gamma-mediated positive energy balance in the rat is associated with reduced sympathetic drive to adipose tissues and thyroid status. Endocrinology 2008;149:2121–2130
42. Carter RN, Paterson JM, Tworowska U, et al. Hypothalamic-pituitary-adrenal axis abnormalities in response to deletion of 11beta-HSD1 is strain-dependent. J Neuroendocrinol 2009;21:879–887
43. LeBrasseur NK, Kelly M, Tsao TS, et al. Thiazolidinediones can rapidly activate AMP-activated protein kinase in mammalian tissues. Am J Physiol Endocrinol Metab 2006;291:E175–E181
44. Hattori A, Mawatari K, Tsuzuki S, et al. Beta-adrenergic-AMPK pathway phosphorylates acetyl-CoA carboxylase in a high-epinephrine rat model, SPORTS. Obesity (Silver Spring) 2010;18:48–54
45. Christ-Crain M, Kola B, Lolli F, et al. AMP-activated protein kinase mediates glucocorticoid-induced metabolic changes: a novel mechanism in Cushing's syndrome. FASEB J 2008;22:1672–1683
46. Berggreen C, Gormand A, Omar B, Degerman E, Göransson O. Protein kinase B activity is required for the effects of insulin on lipid metabolism in adipocytes. Am J Physiol Endocrinol Metab 2009;296:E635–E646
47. Kelly IE, Han TS, Walsh K, Lean ME. Effects of a thiazolidinedione compound on body fat and fat distribution of patients with type 2 diabetes. Diabetes Care 1999;22:288–293
48. Yamauchi T, Kamon J, Waki H, et al. The mechanisms by which both heterozygous peroxisome proliferator-activated receptor gamma (PPARgamma) deficiency and PPARgamma agonist improve insulin resistance. J Biol Chem 2001;276:41245–41254
49. Hoene M, Weigert C. The role of interleukin-6 in insulin resistance, body fat distribution and energy balance. Obes Rev 2008;9:20–29
50. Ruderman NB, Keller C, Richard AM, et al. Interleukin-6 regulation of AMP-activated protein kinase. Potential role in the systemic response to exercise and prevention of the metabolic syndrome. Diabetes 2006;55 (Suppl. 2):S48–S54
51. Hoppmann J, Perwitz N, Meier B, et al. The balance between gluco- and mineralo-corticoid action critically determines inflammatory adipocyte responses. J Endocrinol 2010;204:153–164
52. Hermanowski-Vosatka A, Balkovec JM, Cheng K, et al. 11beta-HSD1 inhibition ameliorates metabolic syndrome and prevents progression of atherosclerosis in mice. J Exp Med 2005;202:517–527
53. Kanda H, Tateya S, Tamori Y, et al. MCP-1 contributes to macrophage infiltration into adipose tissue, insulin resistance, and hepatic steatosis in obesity. J Clin Invest 2006;116:1494–1505

Downloaded from http://diabetes.diabetesjournals.org/diabetes/article-pdf/60/4/1158/401369/1158.pdf by guest on 24 April 2024